Journal of Beijing Institute of Technology, 2021, Vol. 30, Suppl.1

Investigation of Reusable Launch Vehicle Landing Guidance Control with Multiple Sliding Surface Technique

Xin Teng[1], Defu Lin[2], Long Xiao[1,3] and Fengdi Zhang[1,3,✉]

(1. Beijing Aerospace Automatic Control Institute, Beijing 100854, China; 2. Beijing Institute of Technology, Beijing 100081, China; 3. National Key Laboratory of Science and Technology on Aerospace Intelligence Control, Beijing 100854, China)

Abstract: This paper proposes an autonomous approach and landing guidance law for a reusable launch vehicle (RLV) at the specified runway touchdown. With the full nonlinear point-mass dynamics, the multiple sliding surfaces guidance (MSSG) technique is developed for the closed-loop guidance law to guarantee a successful approach and landing (A&L) movement, which has the same advantage in the finite time convergent property as higher order sliding mode control. Its global stability is proved using Lyapunov theory. The resultant guidance law has features in on-line trajectories calculation without any off-line analysis only using the boundary conditions of the A&L phase and instantaneous states of the RLV. Therefore, it is capable of targeting different touchdown points on the runway and overcoming large initial condition errors. Simulations are provided to verify the effectiveness of the proposed law.

Key words: reusable launch vehicle; landing guidance; sliding mode control; finite time

CLC number: TP2 **Document code:** A **Article ID:** 1004-0579(2021)S1-0151-08

Approach and landing (A&L) guidance has recently drawn great attention from researchers in aeronautic industry. A trajectory-planning-based guidance scheme for the A&L phase was developed in Ref.[1], which divides the whole flight profile into several segments. It has been proved that the trajectory-planning guidance method can lead to a successful landing condition even in the presence of severe wind, extreme trajectory dispersions, and aerodynamic uncertainties. In Ref.[2], this approach was further extended to land an RLV with limited normal acceleration capabilities by minimizing the maximal load factor during the A&L phase. With the wide spread use of Optimum-Path-To-Go (OPTG) algorithms[3-5] to the A&L phase, they achieved the online trajectory reshaping and retargeting. These OPTG algorithms can also deal with control surface errors and the terminal area energy management (TAEM) phase[6-7]. Nevertheless, it is infeasible to generate a large amount of off-line trajectories in advance during the process of online trajectory reconfiguration. Nowadays, convex optimization has been used for landing guidance[8-9].

Sliding mode control (SMC) has strong robustness so that it is widely used in the guidance law design[10-13]. For example, the sliding mode terminal guidance (SMTG) was proposed to solve the A&L guidance problem[13]. However, the associated guidance command prevented itself from off-line requirements and was able to generate new trajectories on-line. A novel nonlinear landing guidance scheme has been developed in Ref.[14], based on high-order sliding-mode con-

Received 2020-01-09
✉ Author for correspondence, Ph. D.
E-mail: 18811789446@163.com
DOI: 10.15918/j.jbit1004-0579.20004

trol theory, the proposed multiple sliding surface guidance algorithm has been designed to take advantage of the ability of the system to reach the sliding surface in a finite time. In Ref.[15], an extended state observer based non-singular fast terminal sliding mode control with fixed-time convergence for a vertical take-off and vertical landing (VTVL) reusable launch vehicle has been developed.

Our objective is two-folded: at the stage of the A&L phase, the RLV can softly land at the predetermined runway; and at the final stage, its vertical velocity is minimized through making the path angle reach near-zero. In this paper, a nonlinear closed-form three-dimensional landing guidance law is developed, which can achieve the landing of an RLV even with large initial errors. This law is realized by designing a multiple sliding surface technique (MSST), which considers both the lateral and longitudinal channel. The sliding mode function and its derivative will reach zero by the end of the first sliding mode period, and the second sliding mode is Lyapunov stable in a finite time. Our method features in the advantages of the simple form but with less information, which makes it more suitable for the onboard implementation.

1 Problem Statement and Formulation

This section gives the dynamic model of the RLV in the A&L phase. The A&L phase can be divided into two segments. The first phase is from the approach and landing interface (ALI) to the transition point T, where any possible lateral errors (i.e. initial pointing error and initial position error) would be corrected. The second phase is from the point T, where the velocity vector of the RLV stays in the pitch plane determined by the runway centerline. The responsibility of the second phase is to bring the RLV from its current states to a desirable touchdown movement. Next, from the transition point T, RLV keeps moving in the pitch plane to bring itself from current states to the desirable touchdown movement.

On the account of a flat-Earth model, the three-degree-of-freedom (3DOF) point-mass dynamics of the RLV is given by

$$\dot{x} = \frac{\mathrm{d}x}{\mathrm{d}t} = V\cos\gamma\cos\chi \tag{1}$$

$$\dot{y} = \frac{\mathrm{d}y}{\mathrm{d}t} = V\sin\gamma \tag{2}$$

$$\dot{z} = \frac{\mathrm{d}z}{\mathrm{d}t} = -V\cos\gamma\sin\chi \tag{3}$$

$$\dot{V} = \frac{\mathrm{d}V}{\mathrm{d}t} = -\frac{D}{m} - g\sin\gamma \tag{4}$$

$$\dot{\gamma} = \frac{\mathrm{d}\gamma}{\mathrm{d}t} = \frac{L\cos\mu}{mV} - \frac{g\cos\gamma}{V} \tag{5}$$

$$\dot{\chi} = \frac{\mathrm{d}\chi}{\mathrm{d}t} = -\frac{L\sin\mu}{mV\cos\gamma} \tag{6}$$

where the flight path angle and heading angle are denoted by γ and χ, respectively. The velocity and transition point are represented by V and T, respectively. Note that the initial lateral errors have been corrected at the transition point T and the trajectory will stay in the pitch plane afterwards. The aerodynamic lift and drag are defined as

$$L = qSC_{\mathrm{L}},\ D = qSC_{\mathrm{D}} \tag{7}$$

where $q = \frac{1}{2}\rho V^2$ is the dynamic pressure dependent on the air density ρ and the speed V; S represents the reference area of the vehicle; the lift and drag coefficients are defined as C_{L} and C_{D}, respectively.

The flight time of the A&L phase is, however, usually not the critical problem. The purpose of this phase is the RLV landing with the least possible vertical velocity at the predetermined position. Therefore, the downrange is selected as the independent variable instead of time on account of the downrange being stringently monotonic increasing during the A&L phase. Thus, the system model can be rewritten as

$$y' = \frac{\mathrm{d}y}{\mathrm{d}x} = \frac{\tan\gamma}{\cos\chi} \tag{8}$$

$$z' = \frac{\mathrm{d}z}{\mathrm{d}x} = -\tan\chi \tag{9}$$

$$V' = \frac{\mathrm{d}V}{\mathrm{d}x} = -\frac{D + mg\sin\gamma}{mV\cos\gamma\cos\chi} \tag{10}$$

$$\gamma' = \frac{\mathrm{d}\gamma}{\mathrm{d}x} = \frac{L\cos\mu - ng\cos\gamma}{mV^2\cos\gamma\cos\chi} \tag{11}$$

$$\chi' = \frac{\mathrm{d}\chi}{\mathrm{d}x} = -\frac{L\sin\mu}{mV^2\cos^2\gamma\cos\chi} \tag{12}$$

$$t' = \frac{\mathrm{d}t}{\mathrm{d}x} = \frac{1}{V\cos\gamma\cos\chi} \tag{13}$$

The A&L guidance law in the next section will be formulated based on this new model above. Note that the desired guidance commands are the angle of attack α and the bank angle μ. Besides, the derivative of the flight path angle γ' and the derivative of the heading angle χ' are used as the auxiliary control efforts. By doing so, the desired guidance commands can be accordingly derived from the auxiliary control efforts.

2 Nonlinear Approach and Landing Guidance Law

In this section, a 3-D nonlinear closed-loop guidance scheme is proposed for the A&L phase by using the MSSG. The guidance scheme aims at designing a robust landing-guidance law, with which a successful touchdown can be achieved at the predetermined landing position even when initial condition errors exist. The lateral guidance and longitudinal guidance logic are described in the sequel.

2.1 Lateral guidance logic

According to Section 2, the lateral errors of the RLV should be eliminated at the point T. We define the x-axis parallel to the runway. (x_t, y_t, z_t) and (x_f, y_f, z_f) are assumed to be the inertial coordinate of T and the touchdown point. The desired heading angle χ' should be zero in this way.

From Eq. (9), it is clear to find a one-to-one correspondence between z' and χ'. Motivated by this observation, we design the first sliding surface as

$$S_{a1} = z - z_t - z_t'(x - x_t) \tag{14}$$

Take differentiation on S_{a1} with respect to x yields

$$S_{a1}' = z' - z_t' \tag{15}$$

and the second derivatives of S_{a1} is

$$S_{a1}'' = z'' = -\frac{1}{\cos^2\chi}\chi' \tag{16}$$

where χ' is the control effort.

Based on Ref.[10], and considering Eqs.(14) (15), the second sliding surface is designed as

$$S_{a2} = S_{a1}' + \frac{\lambda S_{a1}}{x_t - x} \tag{17}$$

Remark 1 From Eq. (17), for the lateral guidance problem, the control process cannot be terminated from $x = x_t$ afterwards since the RLV has not yet reached the touchdown point.

Lemma 1 Suppose $x_0 < x_k < x_t$ and $\lambda > 1$ is a constant. If S_{a2} keeps zero from x_k afterwards, both S_{a1} and S_{a1}' will converge to zero at $x = x_t$.

Theorem 1 $z \to z_t$, $\chi \to \chi_t$ as $x \to x_t$, for the lateral guidance system specified in Eq.(9), Eq.(16) under the guidance law(18):

$$\chi' = \cos^2\chi\left[\left(\frac{\lambda S'_{a1}}{x_t - x} + \frac{\lambda S_{a1}}{(x_t - x)^2}\right) + \frac{|S_{a2}(x_0)|}{x_k}\operatorname{sgn}(S_{a2})\right] \tag{18}$$

The cross range z and the heading angle will converge to their expectation as $x \to x_t$.

Proof Define the following Lyapunov candidate

$$V_1 = \frac{1}{2}S_{a2}^2 \tag{19}$$

The derivative of V_1 with respect to the downrange can be calculated as

$$V_1' = S_{a2}S_{a2}' = S_{a2}\left(S_{a1}'' + \frac{\lambda S_{a1}'}{(x_t - x)^2} + \frac{\lambda S_{a1}}{(x_t - x)^2}\right) = S_{a2}\left(-\frac{1}{\cos^2\chi}\chi' + \frac{\lambda S_{a1}'}{x_t - x} + \frac{\lambda S_{a1}}{(x_t - x)^2}\right) \quad (20)$$

Then, substituting the guidance command Eq. (18) into Eq. (20), yields

$$V_1' = S_{a2}\left(-\frac{|S_{a2}(x_0)|}{x_k}\operatorname{sgn}(S_{a2})\right) = -\frac{|S_{a2}(x_0)|}{x_k}|S_{a2}| < 0 \quad (21)$$

According to the Lyapunov theory, the system is globally stable. Further, from Eq. (21), we have $S_{a2}' = -\dfrac{|S_{a2}(x_0)|}{x_k}\operatorname{sgn}(S_{a2})$, which implies that $\dfrac{|S_{a2}(x_0)|}{x_k}$ denotes the rate of approaching the second sliding surface. Consequently, S_{a2} would reach zero at the downrange of x_k and maintain thereafter. Associating this result with Lemma 1, it can be concluded that both S_{a1} and S_{a1}' would go to zero as $x \to x_t$. When x converges to x_t on the second sliding surface, i.e., $S_{a2}=0$, S_{a1} and S_{a1}' will accordingly become zero. Therefore, it can be concluded from Eqs. (14) (15) that z and χ converges to their expected values, respectively.

However, the cross range z and heading angle χ should be reached by applying the guidance in the region of $x_t \le x \le x_f$. In the following, this issue will be addressed.

Suppose that $\triangle x$ is small and positive. The second sliding surface is derived as below in case $x_t - \triangle x \le x \le x_f$.

$$S_{a2} = S_{a1}' + \frac{\lambda}{\Delta x}S_{a1} \quad (22)$$

Note that S_{a2} is continuous at $x = x_t - \triangle x$. By substituting $S_{a2}=0$ into Eq. (22), it can be obtained as

$$\begin{aligned} S_{a1} &= k_1 e^{-k_2[x-(x_t-\Delta x)]} \\ S_{a1}' &= -k_1 k_2 e^{-k_2[x-(x_t-\Delta x)]} \end{aligned} \quad (23)$$

where both $k_1 = S_{a1}(x_t - \triangle x)$ and $k_2 = \dfrac{\lambda}{\triangle x}$ are constants.

From Eq. (23), it is obvious that S_{a1} and S_{a1}' are continuous at $x = x_t - \triangle x$ and monotonically decreasing when $x \ge x_t - \triangle x$. Therefore, we can obtain the desired values of z and χ, since S_{a1} and S_{a1}' are both constrained within a small vicinity of origin when $x_t - \triangle x \le x \le x_f$.

Therefore, by considering $V_2 = S_{a2}^2/2$, we can derive the lateral guidance command for $x_t - \triangle x \le x \le x_f$ using Lyapunov Second Method. The final lateral guidance command is formulated as

$$\chi' = \begin{cases} \cos^2\chi\left[\left(\dfrac{\lambda S'_{a1}}{x_t - x} + \dfrac{\lambda S_{a1}}{(x_t - x)^2}\right) + \dfrac{|S_{a2}(x_0)|}{x_k}\operatorname{sgn}(S_{a2})\right], (\mathrm{A}) \\ \cos^2\chi\left(\dfrac{\lambda S'_{a1}}{\Delta x} + \dfrac{|S_{a2}(x_0)|}{x_k}\operatorname{sgn}(S_{a2})\right), (\mathrm{B}) \end{cases} \quad (24)$$

where (A) is for $x_0 \leqslant x \leqslant x_t - \triangle x$ and (B) is for $x_t - \triangle x \leqslant x \leqslant x_f$.

2.2 Longitudinal guidance logic

The longitudinal guidance logic aims to ensure a soft landing for the RLV at the touchdown point. The flight path angle and vertical velocity at the touch down are denoted by γ_f and V_{yf}, respectively. If γ_f is approaching zero, a minimal magnitude of V_{yf} can be thus ensured. Therefore, we establish the first sliding surface as below

$$\begin{aligned} S_{b1} &= y - y_f - y_f'(x - x_f) \\ S_{b1}' &= y' - y_f' \end{aligned} \quad (25)$$

where y_f' is final value of y', i.e., $\dfrac{\tan\gamma_f}{\cos\chi_t}$.

With $\chi = \chi_t$ for $x_t \le x \le x_f$, it is obvious to verify that both S_{b1} and S_{b1}' remain zero, and $y \to y_f$ as $x \to x_f$. Therefore, a second sliding surface is designed as

$$S_{b2} = S_{b1}' + \frac{\lambda S_{b1}}{x_f - x} \quad (26)$$

Theorem 2 For the longitudinal guidance system as in Eqs. (8) (25), if $x_0 < x_l < x_f$, we have $y \to y_f$ and $\gamma \to \gamma_f$ as $x \to x_f$.

$$\gamma' = -\chi'\sin\gamma\cos\gamma\tan\chi - \cos^2\gamma\cos\chi\cdot\left[\frac{\lambda S'_{b1}}{x_f - x} + \frac{\lambda S_{b1}}{(x_f - x)^2} + \frac{|S_{b2}(x_0)|}{x_t}\operatorname{sgn}(S_{b2})\right] \quad (27)$$

Proof The proof is similar to that of Theorem 1 by choosing $V_3 = \frac{1}{2}S_{b2}^2$ as the Lyapunov function.

Remark 2 By Eq. (27), there will result in a singular problem as $x_f \to x$ appears in the denominator, and this can be solved if $\lambda > 2$ is chosen, i.e.,

$$\gamma' = -\chi' \sin\gamma\cos\gamma\tan\chi - \cos^2\gamma\cos\chi \cdot \left[\lambda b_1 (x_f - x)^{\lambda-2}(1-\lambda) + \frac{|S_{b2}(x_0)|}{x_t}\mathrm{sgn}(S_{b2})\right] \tag{28}$$

Remark 3 When the associated first sliding surface and its derivative reach zero, the longitudinal guidance process terminates while the lateral guidance process still continues. Therefore, the longitudinal control scheme can effectively reach a control objective within a given finite time, while the lateral control aims at tracking problems. Finally, the state errors converges zero within a given finite time and remains this state thereafter.

2.3 Angle of attack and bank angle commands

The lateral and longitudinal guidance commands in the previous section can be deduced from the system of Eqs. (8)–(13). Note that, by the following transformation, the guidance commands can also be transformed into the time domain by

$$\frac{\mathrm{d}(\cdot)}{\mathrm{d}t} = \frac{\mathrm{d}(\cdot)}{\mathrm{d}x}\frac{\mathrm{d}x}{\mathrm{d}t} \tag{29}$$

Therefore, the guidance commands are time-varying and can be rewritten as

$$\begin{aligned}\dot{\chi} &= \chi' V\cos\gamma\cos\chi \\ \dot{\gamma} &= \gamma' V\cos\gamma\cos\chi\end{aligned} \tag{30}$$

The simulation is therefore conducted based on the system described by Eqs. (1)–(6). The angle of attack and bank angle commands will be formulated as follows.

By using Eqs. (5) (6), the bank angle command can be given by

$$\mu = a\tan\frac{-V\dot{\chi}\cos\gamma}{V\dot{\gamma} + g\cos\gamma} \tag{31}$$

Then, by using Eqs. (5) (7), the commanded lift coefficient C_{Lc} is calculated by

$$C_{\mathrm{Lc}} = \frac{m(V\dot{\gamma} + g\cos\gamma)}{qS\cos\mu} \tag{32}$$

Consequently, the angle of attack command can be derived by using Newton's method, linear interpolation or other numerical methods[16-17].

3 Simulation and Results

In this section, numerical simulations are conducted to study the guidance law. The RLV model used for simulations can be referred to Ref.[10]. The lift and drag coefficients can be determined by

$$C_{\mathrm{Lc}} = C_{\mathrm{L0}}a,\ C_{\mathrm{D}} = C_{\mathrm{D0}} + K_{\mathrm{I}}C_{\mathrm{L}}^2 \tag{33}$$

where α is angle of attack; C_{L0} and C_{D0} are initial values of the lift and drag coefficients; K_{I} is the gain for drag coefficient (Tab. 1).

Tab. 1 Parameters of model

Parameter name	Value
S/m	0.912 ft^2/slug
C_{L0}	2.3
C_{D0}	0.0975
K_{I}	0.1819

Furthermore, the parameters x_t, x_k, x_l in the numerical simulations are formulated as

$$x_t = kx_t(x_f - x_0) + x_0 \tag{34}$$

$$x_k = kx_k(x_t - x_0) + x_0 \tag{35}$$

$$x_l = kx_l(x_f - x_0) + x_0 \tag{36}$$

The study uses the atmospheric characteristics of the U. S. in 1976, the standard atmosphere[18]. The parameters for each simulation are detailed in Tab. 2. The allowable angle of attack is bounded within (–10°, 30°).

Tab. 2 Parameters of model

Item	Initial	Final	Parameter	Value
x	0 ft	2×10^4 ft	kx_t	0.5
y	1×10^4 ft	0	kx_k	0.4
z	500 ft	0	kx_l	0.6
γ	–25°	–0.5°	Δx	1.0
χ	0°	0°	λ	3.0

This paper introduces the boundary layer technique to eliminate the chattering problem caused by the switch function

$$\text{sat}(s) = 2\left(\frac{1}{1+\text{e}^{-as}} - \frac{1}{2}\right), a > 0 \qquad (37)$$

Take $a = 0.001$ because the smaller the boundary layer is, the higher control precision will be, but if it is too small, it cannot eliminate the chattering problem.

Simulations for three different conditions are carried out to verify the effectiveness of the multiple sliding surface guidance technique.

Case I Effect of the altitude and cross range

From Figs. 1–6, we can see MSSG can generate effective guidance instructions to guarantee a soft landing of RLV with different initial height error as well as initial cross range. It can be observed that the heading angle χ can converge to zero at the transition point T and bank angle converge to zero in the end. Fig. 7 and Fig. 8 show that the MSSG is still valid in discontinuous slope when the two sliding functions S_{a2} and S_{i2} converge to 0.

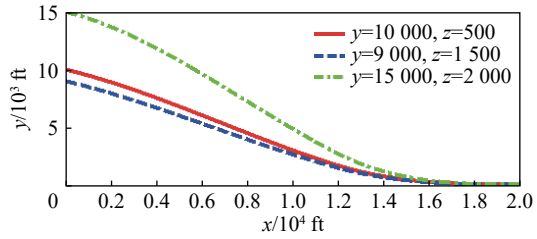

Fig. 1 Downrange and altitude

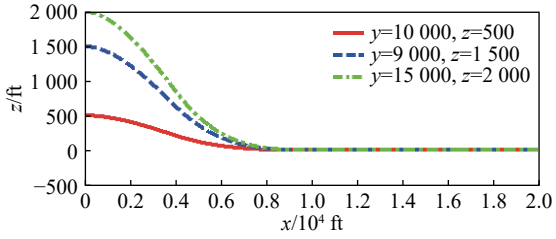

Fig. 2 Downrange and crossrange

Case II Effect of the flight path angle and heading angle

As shown from Fig.10 to Fig. 12, the flight path angle γ and initial heading angle χ can be successfully adjusted to the desired values even subject to obvious pull behavior. Also, from Fig.9 to Fig. 11, the RLV can achieve the soft landing in predefined degree (–0.5°) under different flight path angles. Smooth guidance is presented in Fig.12 to Fig. 14, which can help attitude tracking system.

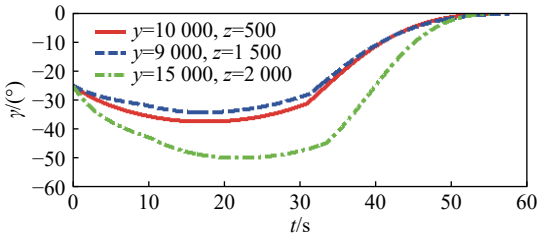

Fig. 3 Time and flight path angle

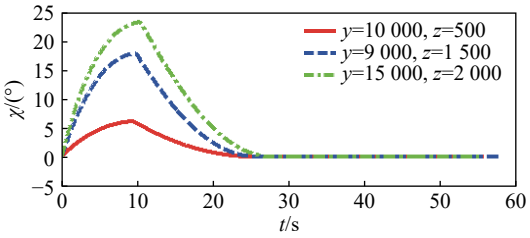

Fig. 4 Time and heading angle

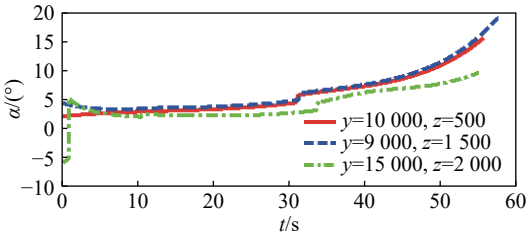

Fig. 5 Time and angle of attack

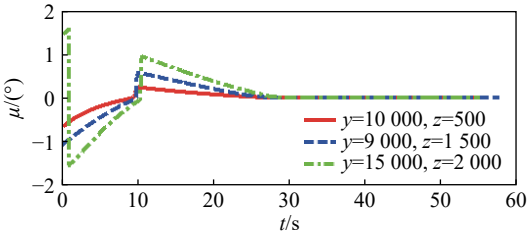

Fig. 6 Time and bank angle

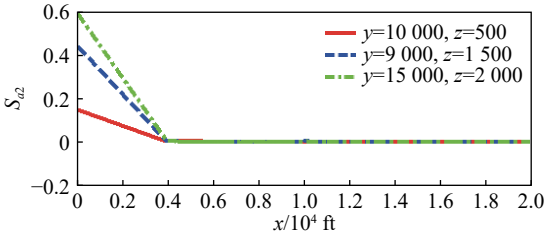

Fig. 7 Downrange and sliding mode surface (S_{a2})

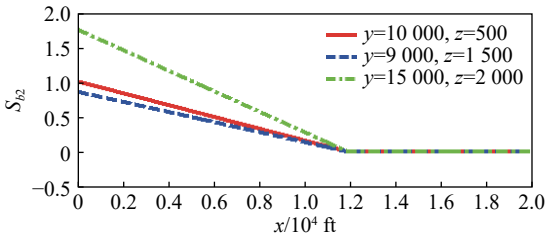

Fig. 8 Downrange and sliding mode surface (S_{b2})

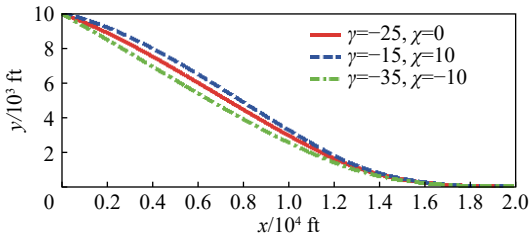

Fig. 9 Downrange and altitude

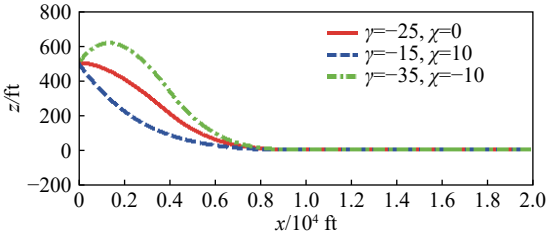

Fig. 10 Downrange and crossrange

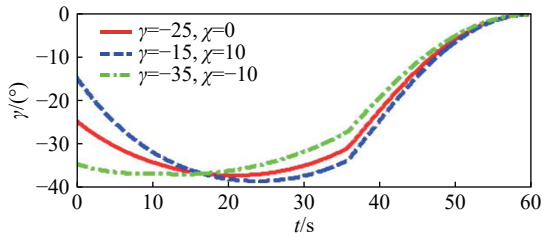

Fig. 11 Time and flight path angle

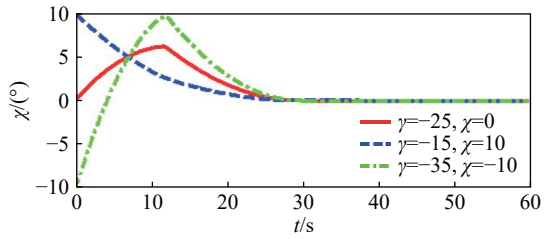

Fig. 12 Time and heading angle

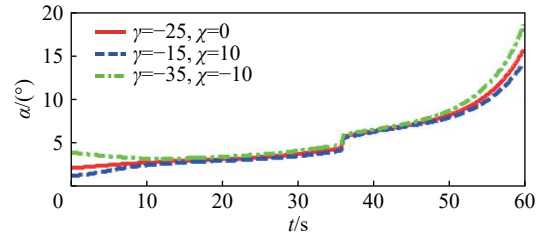

Fig. 13 Time and angle of attack

Our guidance law shows strong robustness against the deviation of initial parameters, which is verified through the above two simulations. As we can observe, the RLV can always land on the accurate orbit no matter what the initial position is. Moreover, the proposed MSSG can produce a visible landing trajectory as the angles change.

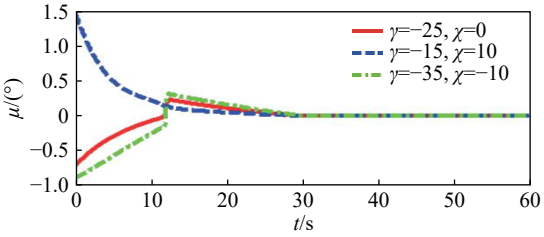

Fig. 14 Time and bank angle

4 Conclusion

This paper proposes a closed-loop guidance control law based on sliding mode control with multiple sliding surface, which thus guarantees a successful A&L movement. The proposed guidance control law is applicable for the RLV in the autonomous approach and landing phase along the predefined orbit. Furthermore, the flight path angle in the final phase gradually approaches to zero for a soft landing so that a smaller vertical velocity is achieved. By using this guidance law, it is remarkable that there is no need for off-line analysis but achieve verification online with a new trajectory.

References:

[1] Kluever C A. Unpowered approach and landing guidance using trajectory planning [J]. Journal of Guidance, Control, and Dynamics, 2004, 27(6): 967-974.

[2] Kluever C A. Unpowered approach and landing guidance with normal acceleration limitations [J]. Journal of Guidance, Control, and Dynamics, 2007, 30(3): 882-885.

[3] Schierman J D, Ward D G, Monaco J F, et al. A reconfigurable guidance approach for reusable launch vehicles[C]// Proceedings of the 2001 AIAA Guidance, Navigation, and Control Conference, 2001.

[4] Schierman J D, Hull J R, Ward D G. Adaptive guidance with trajectory reshaping for reusable launch vehicles[C]// Proceedings of the 2002 AIAA Guidance, Navigation, and Control Conference, 2002.

[5] Schierman J D, Hull J R, Ward D G. On-line trajectory command reshaping for reusable launch vehicles[C]// Proceedings of the 2003 AIAA Guidance, Navigation, and Control Conference, 2003.

[6] Schierman J D, Ward D G, Hull J R, et al. Integrated adaptive guidance and control for re-entry vehicles with flight test results [J]. Journal of Guidance, Control, and Dynamics, 2004, 27(6): 975-988.

[7] Schierman J D, Hull J R. In-flight entry trajectory optimization for reusable launch vehicles[C]// Proceedings of the 2005 AIAA Guidance, Navigation, and Control Conference, 2005.

[8] Szmuk M, Eren U, Acikmese B. Successive convexification for mars 6-dof powered descent landing guidance[C]// AIAA Guidance, Navigation, and Control Conference, 2017: 1500.

[9] Wang J, Cui N, Wei C. Optimal rocket landing guidance using convex optimization and model predictive control [J]. Journal of Guidance, Control, and Dynamics, 2019, 42(5): 1078-1092.

[10] Heydari A, Balakrishnan S N. Path planning using a novel finite horizon suboptimal controller [J]. Journal of Guidance, Control, and Dynamics, 2013, 36(4): 1210-1214.

[11] Menon P K, Vaddi S S, Sengupta P. Robust landing guidance law for impaired aircraft [J]. Journal of Guidance, Control, and Dynamics, 2012, 35(6): 1865-1877.

[12] Su X, Liu X, Shi P, et al. Sliding mode control of discrete-time switched systems with repeated scalar nonlinearities [J]. IEEE Transactions on Automatic Control, 2016, 62(9): 4604-4610.

[13] Harl N, Balakrishnan S N. Reentry terminal guidance through sliding mode control [J]. Journal of Guidance, Control, and Dynamics, 2010, 33(1): 186-199.

[14] Furfaro R, Cersosimo D, Wibben D R. Asteroid precision landing via multiple sliding surfaces guidance techniques [J]. Journal of Guidance, Control, and Dynamics, 2013, 36(4): 1075-1092.

[15] Zhang L, Wei C, Wu R, et al. Fixed-time extended state observer based non-singular fast terminal sliding mode control for a VTVL reusable launch vehicle [J]. Aerospace Science and Technology, 2018, 82: 70-79.

[16] Li M M, Hu J. An approach and landing guidance design for reusable launch vehicle based on adaptive predictor–corrector technique [J]. Aerospace Science and Technology, 2018, 75: 13-23.

[17] Zhao Y, Sheng Y Z, Liu X D, et al. Analytic approach and landing guidance through a novel time-varying sliding mode control method [J]. Journal of Aerospace Engineering, 2016, 29(4): 1-11.

[18] US COESA, Committee on Extension to the Standard Atmosphere. US Standard Atmosphere 1976, NOAA-S/T 76-1562[R]. Washington, DC: US Gov. Printing Office, Sup. DOCS, 1976.